Available online at www.sciencedirect.com
ScienceDirect
Trans. Nonferrous Met. Soc. China 29(2019) 1430−1438
Transactions of Nonferrous Metals Society of China
www.tnmsc.cn

Microstructure evolution and its effect on flow stress of TC17 alloy during deformation in $\alpha+\beta$ two-phase region

Jiao LUO, Peng YE, Wen-chao HAN, Miao-quan LI

School of Materials Science and Engineering, Northwestern Polytechnical University, Xi'an 710072, China

Received 27 August 2018; accepted 21 May 2019

Abstract: The microstructure evolution and its effect on flow stress of TC17 alloy during deformation in the $\alpha+\beta$ two-phase region were investigated via microstructure characterization and isothermal compression tests. Results showed that the spheroidized rate of α phase at 820 and 850 °C slightly increased with increasing strain. With increasing deformation temperature, the spheroidized rate of α phase showed a slight increasing trend, but the volume fraction of α phase significantly decreased. The flow stress at 780 °C and 1 s^{-1} decreased continuously and steady state condition was not achieved up to strain of 1.2 due to dislocation annihilation and α lamellae rotation. Under this condition, the dynamic spheroidization was retarded. At the deformation temperatures of 820 and 850 °C, and a strain rate of 1 s^{-1}, a steady state flow stress was observed at strains above 0.8 due to the balance between work hardening and dynamic softening. The dynamic softening was attributed to the α lamellae rotation, dynamic recovery and a little spheroidization.

Key words: TC17 alloy; spheroidized rate; microstructure evolution; flow stress; microstructure characterization

1 Introduction

The microstructure of titanium alloys is very sensitive to processing parameters during high deformation temperature. Microstructure evolution, such as substructure evolution, grain growth, and dynamic recovery/recrystallization, often alternately or simultaneously occurs during high deformation temperature, and dynamically affects the flow stress and determines the mechanical properties of alloys. Therefore, it is necessary to investigate the microstructure evolution and flow behavior of titanium alloys.

In the past several years, a number of researchers have paid much attention to the relationships between the flow behavior and the microstructure evolution of titanium alloys [1,2]. For instance, GHASEMI et al [3] noted that dynamic recrystallization (DRX) occurred at 1000 °C and 0.1 s^{-1} during isothermal compression of BT9 titanium alloy, while dynamic recovery (DRV) occurred as the major microstructure mechanism under other conditions. Microstructure evolution resulted in two distinct flow curves: one showed a peak followed by a gradual decrease to a steady state stress (DRX) and the other showed a gradual increase to a peak followed by a steady state stress (DRV). LI et al [4] found that platelet spheroidization was beneficial to flow softening of material during hot deformation of TC6 alloy. JING et al [5] established the rapid drop and subsequent oscillation of the flow stress for TC11 alloy after the peak stress before true strain of 0.15. This phenomenon was attributed to the generation of new β phase due to the stress-induced $\alpha\rightarrow\beta$ phase transformation.

Although the relationship between the flow behavior and microstructure evolution of titanium alloys with an equiaxed microstructure had been investigated, relatively little attention focused on the changes of microstructure variables for titanium alloys with a basketweave microstructure at different processing parameters and their effect on the flow behavior. The basketweave microstructure of two-phase titanium alloys could be processed to produce a globular one in the $\alpha+\beta$ two-phase region by deformation and to give a good strength and ductility [6]. Therefore, it is necessary to study the microstructure evolution of titanium alloys

Foundation item: Project (51575446) supported by the National Natural Science Foundation of China; Project (2017KJXX-27) supported by the Shaanxi Province Youth Science and Technology New Star Plan, China; Project (3102017AX003) supported by the Fundamental Research Funds for the Central Universities, China

Corresponding author: Jiao LUO; Tel: +86-29-88460465; E-mail: luojiao@nwpu.edu.cn

DOI: 10.1016/S1003-6326(19)65050-8

with a basketweave microstructure and its effect on the flow stress to control the microstructure and require ideal properties.

In this study, TC17 (Ti−5Al−2Sn−2Zr−4Mo−4Cr) alloy with a basketweave microstructure was selected as the experimental material. This "beta-rich" $\alpha+\beta$ type titanium alloy has high strength and high toughness, which makes it an ideal material for gas turbine engine components, such as shaft disks, blades, and casings [7−12]. The objective of this work is to quantitatively investigate the effect of the deformation temperature and strain on the microstructure evolution at a higher strain rate and to discuss the effect of microstructure evolution on the flow stress of TC17 alloy with a basketweave microstructure in the $\alpha+\beta$ two-phase region. For this purpose, isothermal compression was carried out at different deformation temperatures and strains. Characterization techniques, including scanning electron microscopy (SEM), transmission electron microscopy (TEM), and high-resolution electron backscatter diffraction (EBSD), were used in the present work.

2 Experimental

2.1 Materials

TC17 alloy with a basketweave microstructure was used in this work. Its measured composition (in wt.%) is 5.12 Al, 2.03 Sn, 2.10 Zr, 4.04 Mo, 3.94 Cr, 0.10 Fe, 0.012 C, 0.007 N, 0.007 H and 0.12 O, balance Ti. The β transus temperature of the alloy was approximately 905 °C. The microstructure of the as-received TC17 alloy taken from a longitudinal section of a bar is shown in Fig. 1. It is observed that the microstructure consists of interwoven α lamellae (marked with red arrows) and β phase (marked with a white arrow), suggesting its basketweave microstructure.

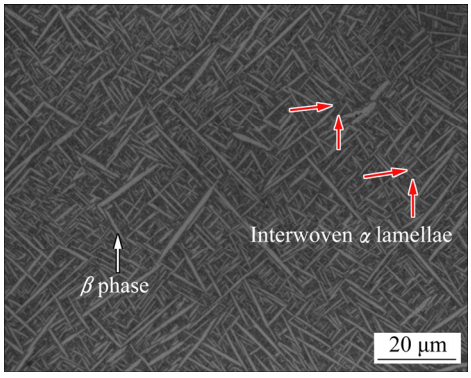

Fig. 1 Basketweave microstructure of TC17 alloy

2.2 Experimental procedures

To investigate the effect of the deformation temperature and strain on the microstructure evolution of TC17 alloy with a basketweave microstructure, isothermal compression was performed using the a Gleeble−3500 simulator at deformation temperatures of 780, 820 and 850 °C, with strains of 0.2, 0.35, 0.9 and 1.2, at a strain rate of 1 s^{-1}. To maintain the microstructure at different strains, the isothermal compression was stopped at each given strain. Samples with size of 8 mm × 12 mm (diameter × height) were heated at a controlled rate of 10 °C/s^{-1}. Upon reaching the deformation temperature, it was maintained for 5 min to establish a uniform temperature in the samples. During isothermal compression, a thermocouple was welded on the surface of the samples to measure the deformation temperature and graphite powder was placed between the specimens and anvils to reduce the die friction. The flow stress−strain curves were recorded automatically in this study. After isothermal compression, the samples were water-quenched to room temperature and sectioned along the diameter to observe the microstructure.

For the SEM and EBSD observations, the samples were mechanically polished and electropolished in a solution containing 6% perchloric acid, 30% butanol and 64% methanol at 16 °C with an applied potential of 20 V. The SEM samples were chemically etched in a solution of 10 mL HF, 15 mL HNO_3 and 75 mL H_2O. A SUPRA 55 SEM operating at 15 kV was used to examine the microstructure at different deformation temperatures and strains. The spheroidized rate, thickness of α lamellae, and volume fraction of α phase were measured using quantitative metallography image analysis software (Image-Pro Plus 6.0) and calculated by the average of 20 visual fields. Here, an α lamella with a Feret ratio below 2 was considered as the spheroidized α, with the spheroidized rate (f) calculated using the equation $f=S_g/S_p$ (where S_g was the total area of spheroidized α and S_p was total area of α phase). The EBSD observation was conducted using a TESCAN MIRA3 XMU high-resolution field emission SEM with an accelerating voltage of 20 kV and step size of 0.1 μm. The EBSD data analysis was performed using an HKL Channel 5 software. The SEM and EBSD micrographs were taken along the direction perpendicular to the compression axis.

For the TEM observation, thin disc samples were prepared by electrical-discharge machining followed by mechanical grinding to a thickness less than 50 μm prior to twin-jet electro-polishing (in a solution of 6% perchloric acid, 30% butanol and 64% methanol at −30 °C with an applied current of 60−80 mA). The TEM micrographs and corresponding selected area diffraction (SAD) patterns of the samples were obtained at 300 kV in an FEI Tecnai F30G^2 TEM. Moreover, all SEM, TEM, and EBSD observations focused on the central (most highly deformed) region of the deformed samples.

3 Results and discussion

3.1 Flow curves and microstructure evolution at different processing parameters

The flow curves of TC17 alloy with a basketweave microstructure compressed at temperatures of 780, 820 and 850 °C and a strain rate of 1 s^{-1} are shown in Fig. 2(a). A sharp increase in the flow stress is observed in the early stage of deformation due to the interaction and multiplication of the dislocations. However, as the dislocation density increases, the rate of dislocation

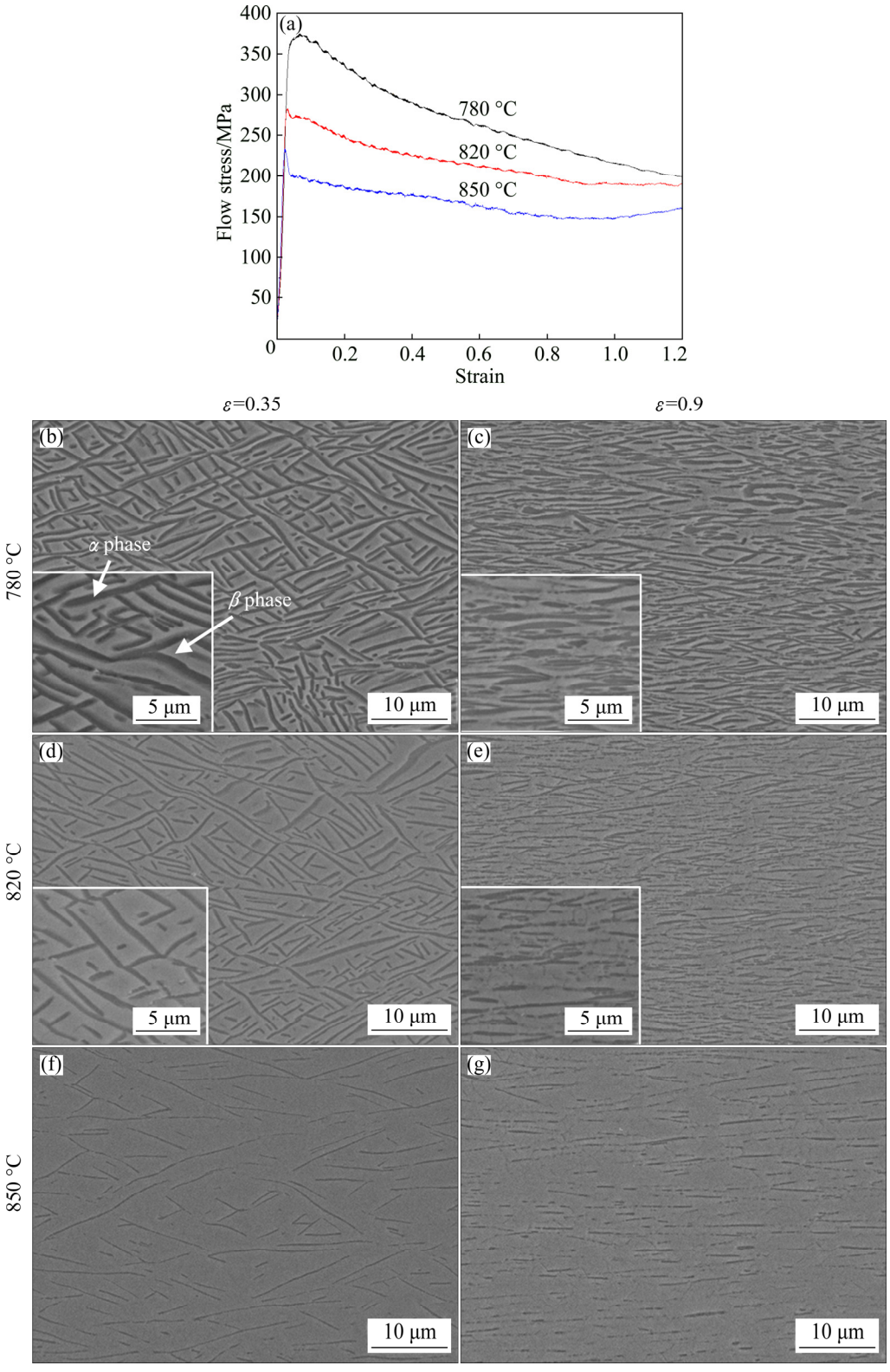

Fig. 2 Flow stress−strain curves of samples deformed at 780, 820, 850 °C and strain rate of 1 s^{-1} (a), and SEM micrographs of deformed TC17 alloy at strains of 0.35 (b, d, f) and 0.9 (c, e, g)

annihilation also increases. This can be explained by the equation of mean dislocation density varing with strain as follows [13,14]:

$$\frac{\mathrm{d}\rho}{\mathrm{d}\varepsilon}=k_1\sqrt{\rho}-k_2\rho \quad (1)$$

where ρ is the dislocation density (cm^{-2}), ε is the strain, k_1 is a constant, and k_2 is the softening parameter, which is a function of temperature and strain rate. In Eq. (1), the rate of dislocation accumulation is proportional to $\rho^{1/2}$, whereas the rate of dislocation annihilation is proportional to ρ. This may cause a decrease in the flow stress as the strain progresses. As shown in Fig. 2(a), the flow curves with an evident softening tendency in the strain range of 0.05−0.8 are consistent with the expected outcome. Particularly, at 780 °C, the flow stress values continuously decrease and the steady state conditions are not observed even until a strain of 1.2. SEMIATIN et al [15] found that flow softening of titanium alloys was related to deformation heating and microstructure evolution. In the present work, the effect of microstructure evolution on the flow stress of TC17 alloy with a basketweave microstructure at a high strain rate was discussed thoroughly.

The SEM micrographs of the deformed TC17 alloy at different strains and deformation temperatures are given in Figs. 2(b−g). Table 1 shows the spheroidized rate and volume fraction of α phase in the deformed TC17 alloy at different strains and deformation temperatures. SUN et al [12] investigated the microstructure of TC17 alloy prior to compression at different heating temperatures and proposed that the α lamellae were still interwoven in the β intragranular regions and retained the basketweave microstructure, but the volume fractions of α phase decreased with increasing temperature. In Fig. 2(b), the microstructure consists of interwoven α lamellae and β phase, with no evident spheroidization behavior observed at a strain of 0.35 and a deformation temperature of 780 °C, which is a similar microstructure to that prior to compression. The spheroidized rate and volume fraction of α phase is (0.5±0.1)% and (31.4±2.0)%, respectively (Table 1). As the strain increases, α lamellae rotate towards the metal flow direction (Fig. 2(c)). The spheroidized rate and volume fraction of α phase at a strain of 0.9 is (0.7±0.1)% and (34.2±2.2)%, respectively. The analysis reveals that the dynamic spheroidization is prominently retarded from (0.4±0.1)% to (0.7±0.2)% at a strain rate of 1 s^{-1} and a deformation temperature of 780 °C and in the strain range of 0.2−1.2. Thus, the sharp flow softening at 780 °C is not attributed to the dynamic spheroidization of α lamellae in TC17 alloy with a basketweave microstructure, which is remarkably different from that obtained by SUN et al [12]. However, the rotation of α lamellae towards the metal flow direction probably leads to a reduction in the flow stress of TC17 alloy due to a low Taylor factors and/or slip transmission across α/β interfaces in this direction [16]. Similarly, the rotation also occurs with increasing strain at else deformation temperatures (820 and 850 °C), as shown in Figs. 2(e) and (g), probably resulting in a reduction in the flow stress of TC17 alloy. Differing from that at 780 °C, the spheroidized rate of α phase at 820 and 850 °C increases in the strain range of 0.2−1.2, as shown in Table 1. This implies that dynamic spheroidization may cause a slight reduction in flow stress of TC17 alloy at 820 and 850 °C except for the effect of lamellar rotation. It is also seen in Table 1 that the strain has negligible influence on the volume fraction of α phase at each deformation temperature. In addition, the volume fraction of α phase decreases from (34.2±2.2)% to (10.3±1.3)% as the deformation temperature decreases from 780 to 850 °C at a strain of 0.9. This suggests that more α lamellae will participate in the lamellar rotation at 780 °C, which leads to a more remarkable trend of flow softening than that of else deformation temperatures. With increasing deformation temperature, the spheroidized rate of α phase shows a slight increasing trend.

Table 1 Spheroidized rate and volume fraction of α phase in deformed TC17 alloy at 780, 820 and 850 °C and strain rate of 1 s^{-1}

Deformation condition	Spheroidized rate of α phase/%	Volume fraction of α phase/%
T=780 °C, $\dot{\varepsilon}$=1 s^{-1}, ε=0.2	0.4±0.1	31.6±2.0
T=780 °C, $\dot{\varepsilon}$=1 s^{-1}, ε=0.35	0.5±0.1	31.4±2.0
T=780 °C, $\dot{\varepsilon}$=1 s^{-1}, ε=0.9	0.7±0.1	34.2±2.2
T=780 °C, $\dot{\varepsilon}$=1 s^{-1}, ε=1.2	0.7±0.2	34.0±2.3
T=820 °C, $\dot{\varepsilon}$=1 s^{-1}, ε=0.2	0.5±0.1	23.0±2.6
T=820 °C, $\dot{\varepsilon}$=1 s^{-1}, ε=0.35	0.6±0.1	23.5±2.3
T=820 °C, $\dot{\varepsilon}$=1 s^{-1}, ε=0.9	3.6±0.4	24.8±2.4
T=820 °C, $\dot{\varepsilon}$=1 s^{-1}, ε=1.2	3.9±0.3	23.0±2.5
T=850 °C, $\dot{\varepsilon}$=1 s^{-1}, ε=0.2	0.6±0.2	10.7±1.8
T=850 °C, $\dot{\varepsilon}$=1 s^{-1}, ε=0.35	0.7±0.3	8.9±1.2
T=850 °C, $\dot{\varepsilon}$=1 s^{-1}, ε=0.9	4.3±0.4	10.3±1.3
T=850 °C, $\dot{\varepsilon}$=1 s^{-1}, ε=1.2	4.6±0.4	9.1±1.2

As seen in Fig. 2(a), the flow stress of TC17 alloy with a basketweave microstructure decreases with increasing deformation temperature. This phenomenon is explained with the aid of the constitutive model coupled with microstructure variables [14,17] in the following equations:

$$\sigma=M\tau \quad (2)$$

$$\tau = n_1 f_\alpha(\tau_\alpha^* + \tau_{\alpha\mu}) + n_2 f_\beta \tau_\beta^* \quad (3)$$

$$\tau_{\alpha\mu} = a\mu(T)b\sqrt{\rho} + kl_\alpha^{-1/2} \quad (4)$$

where σ is the flow stress (MPa), M is the Taylor factor (3.06), τ is the shear stress (MPa), f_α and f_β are the volume fractions of α phase and β phase, respectively, with $f_\alpha+f_\beta=1$, n_1 and n_2 are weight coefficients, τ_α^* and τ_β^* are the thermally activated stresses of α phase and β phase (MPa), respectively, $\tau_{\alpha\mu}$ is the athermal stress of α phase associated with strain hardening and grain boundary strengthening (MPa), b is the Burgers vector magnitude (2.86×10^{-10} m), a and k are material constants, $\mu(T)$ is the temperature-dependent shear modulus, and l_α is the average thickness of α lamellae (μm).

The constitutive model indicates the increase of the flow stress for titanium alloys when the volume fraction of α phase increases and the thickness of α lamellae decreases. Comparing Fig. 2(b) with (d), the volume fraction of the α phase decreases from (31.4±2.0)% to (23.5±2.3)% due to the $\alpha\rightarrow\beta$ phase transformation, but the thickness of α lamellae has not significantly change in the temperature range. Thus, the flow stress of TC17 alloy with a basketweave microstructure decreases due to the combined effects of these aspects. At 850 °C (Fig. 2(f)), the volume fraction of α phase decreases continuously to be (8.9±1.2)%, which further promotes a decrease in the flow stress of TC17 alloy. The above results and analyses indicate that the microstructure evolution (lamellar rotation and volume fraction of α phase) profoundly affects the flow stress of TC17 alloy with a basketweave microstructure at a high strain rate. The dynamic spheroidization has a slight effect on the flow stress at some deformation temperatures and α lamellae thickness has a negligible effect on the flow stress.

3.2 Microstructure evolution and its effect on flow stress

Microstructure evolution of TC17 alloy in the $\alpha+\beta$ two-phase region is further elucidated via TEM and EBSD observations shown in Figs. 3−5. At a deformation temperature of 820 °C, a strain rate of 1 s^{-1} and a strain of 0.35, the microstructure is composed of thin α lamellae with a thickness of approximately 250 nm and β phase (Fig. 3(a)). The thin α lamellae are interwoven and separated by thick laths of β phase. In some α lamellae interiors, the dislocation density is very high (Fig. 3(b)), specifically the dislocation walls/cells and tangles form at the intersections of α lamellae (Fig. 3(c)), which is a distinct evidence of work hardening. By increasing the strain, these walls/cells decrease in size to minimize the stored energy and the cell boundaries sharpen and recover into highly disoriented sub-boundaries. The formation of recovered sub-boundaries promotes a decrease of flow stress for TC17 alloy with a basketweave microstructure, which results in a dynamic equilibrium of the work hardening and recovery rates at a certain strain; the dislocation density remains constant and a steady-state flow stress is obtained [18]. A detailed evidence on the formation of recovered sub-boundaries in TC17 alloy with a basketweave microstructure at a larger strain is provided in the following section. In addition, a very

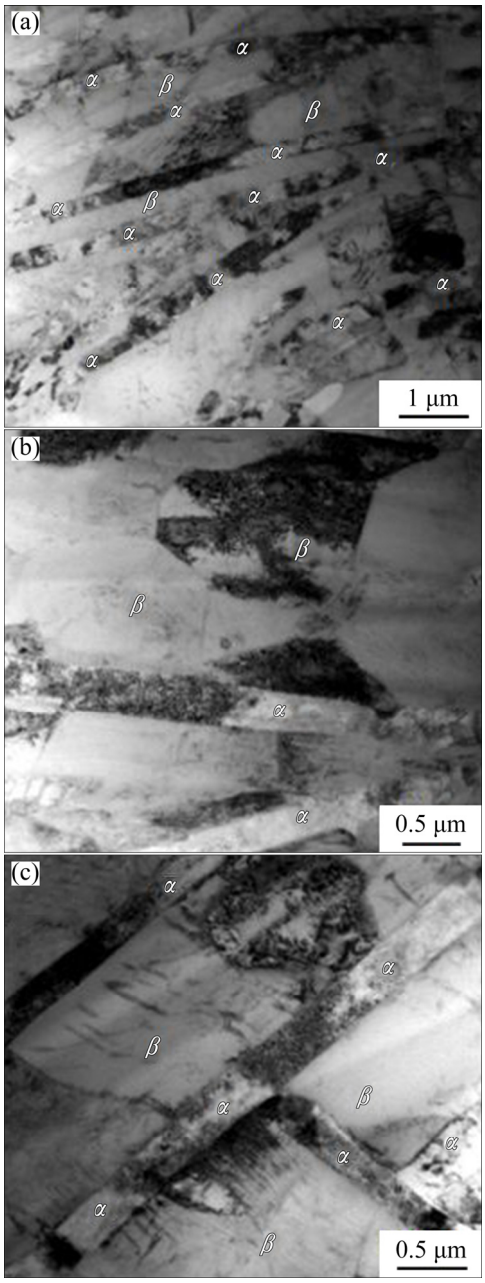

Fig. 3 TEM micrographs of samples at deformation temperature of 820 °C, strain rate of 1 s^{-1} and strain of 0.35: (a) Interwoven α laths; (b, c) Dislocation walls

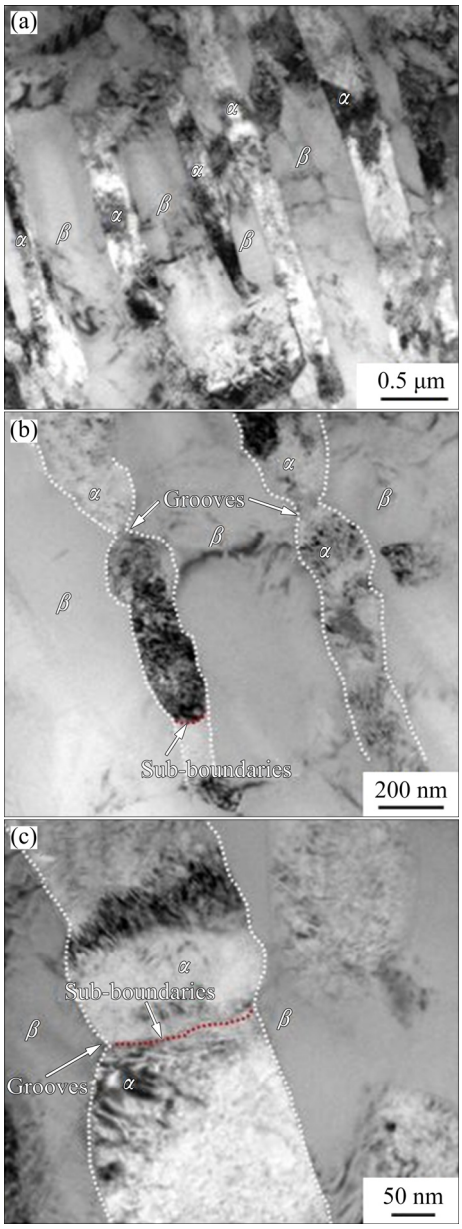

Fig. 4 TEM micrographs of samples at deformation temperature of 820 °C, strain rate of 1 s^{-1} and strain of 1.2: (a) Parallel α laths; (b, c) Sub-boundaries

high dislocation density is observed within β phase (Fig. 3(b)), implying that the soft β phase also participates in plastic deformation, and the recovered sub-boundaries are also present in it. Therefore, work hardening in TC17 alloy is dominated in the early deformation stage.

With increasing strain (Fig. 4(a)), α lamella rotation predominantly occurs and is perpendicular to the compression direction. Thus, the occurrence of more lamella rotation causes reduction in the flow stress of TC17 alloy with a basketweave microstructure in the α+β two-phase region. In addition, Figs. 4(b) and (c) show highly irregular α/β boundaries, with grooves at the intersections of the intraphase α/α boundaries and interphase α/β boundaries. Recovered sub-boundaries are also observed in the thin α lamellae interiors, which result in a decreased flow stress with increasing strain except for the lamella rotation. Moreover, the sub-boundaries have an important role in the spheroidization process. Previous references [19,20] reported that spheroidization by boundary-splitting mechanism required an internal boundary through the thickness of one of the lamellar phases. The recovered sub-boundary is a possible resource that creates an unstable dihedral angle (90°). Subsequently, this dihedral angle reduces to minimize the surface tension, resulting in the formation of the grooves at the intersections of the intraphase α/α boundaries and interphase α/β boundaries (Figs. 4(b) and (c)). The formation of grooves promotes fragmentation and spheroidization of α lamellae in TC17 alloy with a basketweave microstructure. The above results and analyses indicate that the flow softening of TC17 alloy with a basketweave microstructure at a deformation temperature of 820 °C, a strain rate of 1 s^{-1} and a strain of 1.2 is attributed to the lamella rotation, recovery of dislocation substructure, and dynamic spheroidization. Thereby, the dislocation density remains constant and a steady-state flow stress is obtained at this strain, being consistent with the expectation in Fig. 2(a).

At a deformation temperature of 850 °C, a strain rate of 1 s^{-1} and a strain of 0.35, the TEM micrographs of TC17 alloy are shown in Fig. 5. The microstructure at 850 °C is fairly different from that at 820 °C. Comparing Fig. 5(a) with Fig. 3(a), most of α lamellae remain interwoven with an increased distance between them. Moreover, from 820 to 850 °C, the volume fraction of α phase decreases, resulting in a decrease in flow stress of TC17 alloy at a higher deformation temperature. As shown in Fig. 5(b), sporadic kinking in α lamellae is present with high dislocation density. SEMIATIN et al [15] proposed that nucleation sites for spheroidization easily occurred at the kinks in α lamellae. This suggests that the formation of kinking α lamellae is beneficial to the dynamic spheroidization of TC17 alloy. Figure 5(c) shows the dislocation tangles in α lamellae and formation of grooves at the intersection of the α/α interfaces and α/β interfaces. Figure 5(d) shows the SAD pattern of location A in Fig. 5(c), which presents a deviation of 8.5°, confirming the formation of low-angle boundaries (LABs) or even sub-boundaries. These phenomena demonstrate that the boundary-splitting mechanism promotes dynamic spheroidization of α lamellae. In addition, some separated α phases with a size of approximately 220 nm are present under this condition (Fig. 5(e)) with individual dislocation observed

in the spheroidized α phase. This implies that dynamic spheroidization of α lamellae results in a decrease of flow stress of TC17 alloy with a basketweave microstructure, even with a dominant work hardening at a deformation temperature of 850 °C, a strain rate of 1 s^{-1} and a strain of 0.35.

Figure 6 shows the inverse pole figure (IPF) and distribution of grain boundary misorientation for the α and β phases of TC17 alloy at a deformation temperature of 850 °C, a strain rate of 1 s^{-1} and a strain of 0.9. In the IPF, low-angle boundaries (1°−15°) are outlined using white lines, high-angle boundaries (more than 15°) of α and β phases are outlined using aquamarine blue and black lines, respectively, and phase boundaries are outlined using blue lines. The IPF map shows that the interwoven α lamellae are mostly replaced by parallel α lamellae due to the rotation of α lamellae (Fig. 6(a)). Between parallel α lamellae, few equiaxed α grains are observed with a size of approximately 260 nm and without low-angle boundaries in its grain interiors. This suggests the occurrence of dynamic recrystallization at a deformation temperature of 850 °C, a strain rate of 1 s^{-1} and a strain of 0.9. In addition, newly formed high-angle boundaries (HABs) in the range of 60°−90°, marked with aquamarine blue lines are present in prior α lamella interiors, being consistent with the result in Fig. 6(b). For instance, Grain 1 and Grain 2 present a misorientation of 69°, while Grain 2 and Grain 3 present a misorientation of 75°. This suggests that misorientation in prior α lamellae interiors does not exceed 15° in the early deformation stage. By increasing the strain, misorientation across some boundary segments begins to exceed 15°, resulting in the formation of HABs and separation of α lamellae. Lastly, they promote a reduction in the flow stress of TC17 alloy with a basketweave microstructure [21].

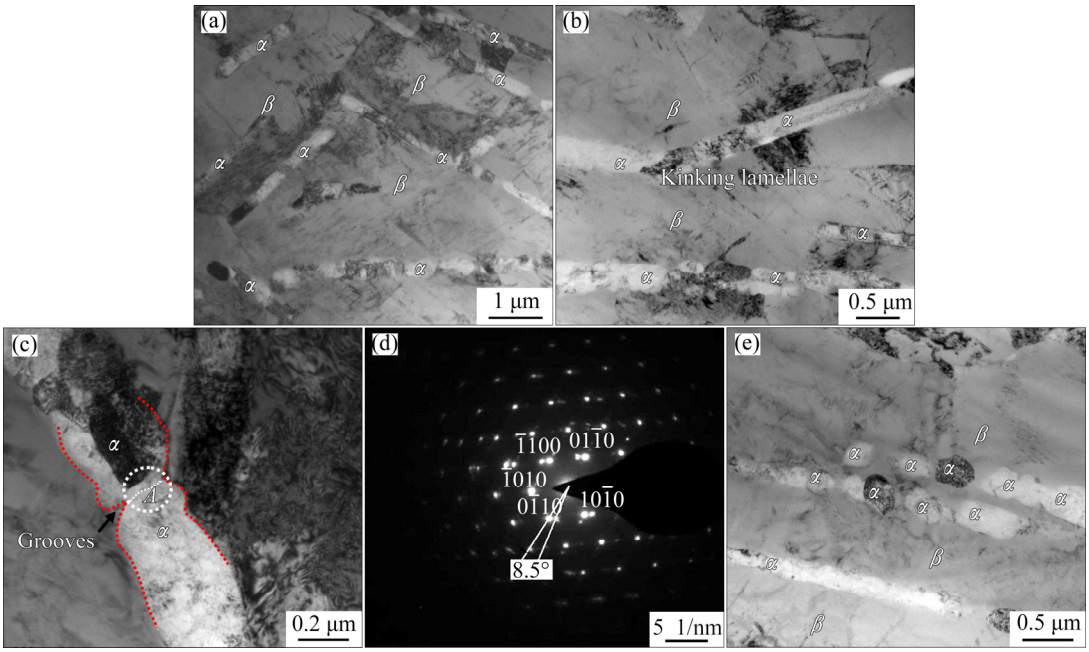

Fig. 5 TEM micrographs of samples at deformation temperature of 850 °C, strain rate of 1 s^{-1} and strain of 0.35: (a) Interwoven α laths; (b) Kinking lamellae; (c) Sub-boundaries; (d) SAD pattern of location A in (c); (e) Equiaxed α grains

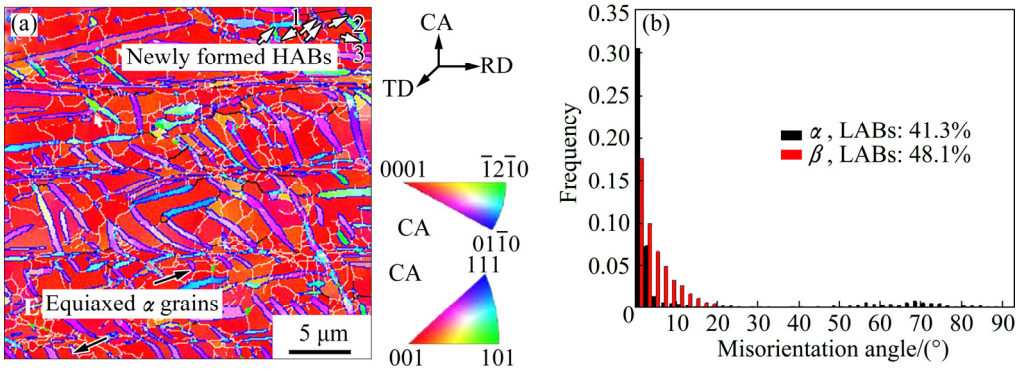

Fig. 6 Inverse pole figure (IPF//CA) (a) and distribution of grain boundary misorientation for α and β phases (b) of TC17 alloy at deformation temperature of 850 °C, strain rate of 1 s^{-1} and strain of 0.9

4 Conclusions

(1) A sharp increase exists in the flow stress of TC17 alloy with a basketweave microstructure during the early stage of deformation due to the dislocation interaction and accumulation. With increasing strain, the flow curves exhibit an evident softening trend.

(2) The spheroidized rate of α phase at 820 and 850 °C slightly increases with increasing strain. This shows a slight increasing trend with increasing deformation temperature.

(3) With increasing deformation temperature, the volume fraction of α phase significantly decreases, resulting in a decreased flow stress. However, the thickness of α lamellae insignificantly changes in the temperature range.

(4) At a deformation temperature of 780 °C and a strain rate of 1 s^{-1}, the flow stress continuously decreases and steady state conditions are not observed up to a strain of 1.2. With increasing strain, an increasing dislocation annihilation rate causes a reduction in the flow stress. In addition, the α lamellae rotation toward the metal flow direction also leads to a decreased flow stress.

(5) At the deformation temperatures of 820, 850 °C and a strain rate of 1 s^{-1}, a steady-state flow stress is observed at strains above 0.8. The α lamellae rotation, recovery of dislocation substructure, and slight spheroidization cause a reduction in flow stress with increasing strain.

References

[1] MIKHAYLOVSKAYA A V, MOSLEH A O, KOTOV A D, KWAME J S, POURCELOT T, GOLOVIN I S, PORTNOY V K. Superplastic deformation behaviour and microstructure evolution of near-α Ti−Al−Mn alloy [J]. Materials Science and Engineering A, 2017, 708: 469−477.

[2] SUN Jin-zhao, LI Miao-quan, LI Hong. Deformation behavior of TC17 titanium alloy with basketweave microstructure during isothermal compression [J]. Journal of Alloys and Compounds, 2018, 730: 533−543.

[3] GHASEMI E, ZAREI-HANZAKI A, FARABI E, TESAŘ K, JÄGER A, REZAEE M. Flow softening and dynamic recrystallization behavior of BT9 titanium alloy: A study using process map development [J]. Journal of Alloys and Compounds, 2017, 695: 1706−1718.

[4] LI Jun-ling, WANG Bao-yu, HUANG He, FANG Shuang, CHEN Ping, SHEN Jin-xia. Unified modelling of the flow behaviour and softening mechanism of a TC6 titanium alloy during hot deformation [J]. Journal of Alloys and Compounds, 2018, 748: 1031−1043.

[5] JING L, FU R D, WANG Y P, QIU L, YAN B. Discontinuous yielding behavior and microstructure evolution during hot deformation of TC11 alloy [J]. Materials Science and Engineering A, 2017, 704: 434−439.

[6] LUO Jiao, YE Peng, HAN Wen-chao, LI Miao-quan. Collaborative behavior in α lamellae and β phase evolution and its effect on the globularization of TC17 alloy [J]. Materials and Design, 2018, 146: 152−162.

[7] XU Jian-wei, ZENG Wei-dong, SUN Xin, JIA Zhi-qiang, ZHOU Jian-hua. Static coarsening behavior of the lamellar alpha in Ti-17 alloy [J]. Journal of Alloys and Compounds, 2015, 631: 248−254.

[8] ZHAO Zhang-long, GUO Hong-zhen, WANG Xiao-chen, YAO Ze-kun. Deformation behavior of isothermally forged Ti−5Al−2Sn−2Zr−4Mo−4Cr powder compact [J]. Journal of Materials Processing Technology, 2009, 209: 5509−5513.

[9] ZHANG Qiang, CHEN Jing, TAN Hua, LIN Xin, HUANG Wei-dong. Microstructure evolution and mechanical properties of laser additive manufactured Ti−5Al−2Sn−2Zr−4Mo−4Cr alloy [J]. Transactions of Nonferrous Metals Society of China, 2016, 26: 2058−2066.

[10] AYED Y, ROBERT C, GERMAIN G, AMMAR A. Orthogonal micro-cutting modeling of the Ti17 titanium alloy using the crystal plasticity theory [J]. Finite Elements in Analysis and Design, 2017, 137: 43−55.

[11] YANG Yang, ZHANG Hua, QIAO Hong-chao. Microstructure characteristics and formation mechanism of TC17 titanium alloy induced by laser shock processing [J]. Journal of Alloys and Compounds, 2017, 722: 509−516.

[12] SUN Jin-zhao, LI Miao-quan, LI Hong. Initial flow softening and restoration mechanisms of isothermally compressed Ti−5Al−2Sn−2Zr−4Mo−4Cr with basketweave microstructure [J]. Materials Science and Engineering A, 2017, 697: 132−140.

[13] DING R, GUO Z X. Microstructural modelling of dynamic recrystallisation using an extended cellular automaton approach [J]. Computational Materials Science, 2002, 23: 209−218.

[14] LUO Jiao, LI Miao-quan, LI Xiao-li, SHI Yan-pei. Constitutive model for high temperature deformation of titanium alloys using internal state variables [J]. Mechanics of Materials, 2010, 42: 157−165.

[15] SEMIATIN S L, SEETHARAMAN V, WEISS I. Flow behavior and globularization kinetics during hot working of Ti−6Al−4V with a colony alpha microstructure [J]. Materials Science and Engineering A, 1999, 263: 257−271.

[16] ZHEREBTSOV S, MURZINOVA M, SALISHCHEV G A, SEMIATIN S L. Spheroidization of the lamellar microstructure in Ti−6Al−4V alloy during warm deformation and annealing [J]. Acta Materialia, 2011, 59: 4138−4150.

[17] GAO Peng-fei, YANG He, FAN Xiao-guang, ZHU Shuai. Unified modeling of flow softening and globularization for hot working of two-phase titanium alloy with a lamellar colony microstructure [J]. Journal of Alloys and Compounds, 2014, 600: 78−83.

[18] HUMPHREYS F J, HATHERLY M. Recrystallization and related annealing phenomena [M]. 2nd ed. Amsterdam: Elsevier, 2004.

[19] MIRONOV S, MURZINOVA M, ZHEREBTSOV S, SALISHCHEV G A, SEMIATIN S L. Microstructure evolution during warm working of Ti−6Al−4V with a colony-α microstructure [J]. Acta Materialia, 2009, 57: 2470−2481.

[20] STEFANSSON N, SEMIATIN S L. Mechanisms of globularization of Ti−6Al−4V during static heat treatment [J]. Metallurgical and Materials Transactions A, 2003, 34: 691−698.

[21] WANG Ke, LI Miao-quan. Characterization of discontinuous yielding phenomenon in isothermal compression of TC8 titanium alloy [J]. Transactions of Nonferrous Metals Society of China, 2016, 26: 1583−1588.

TC17 合金在 $\alpha+\beta$ 两相区变形时的显微组织演变及其对流动应力的影响

罗 皎，叶 鹏，韩文超，李淼泉

西北工业大学 材料学院，西安 710072

摘 要：基于显微组织表征和等温热模拟压缩试验，研究 TC17 合金在 $\alpha+\beta$ 两相区变形时的显微组织演变及其对流动应力的影响。研究表明：当变形温度为 820 和 850 °C 时，随着应变的增加，α 相的球化率略微增加；随着变形温度的升高，α 相的球化率略微增加，但是 α 相的体积分数明显减小。当变形温度为 780 °C、应变速率为 1 s^{-1} 时，流动应力呈减小趋势；当应变为 1.2 时，由于位错湮没和 α 片层转动，流动应力未达到稳定状态。当变形温度为 820 和 850 °C、应变速率为 1 s^{-1}、应变大于 0.8 时，由于加工硬化和动态软化的平衡作用，流动应力呈稳定状态。合金动态软化归因于 α 片层转动、动态回复和轻微的球化。

关键词：TC17 合金；球化率；显微组织演变；流动应力；显微组织表征

(Edited by Wei-ping CHEN)